Journal of Alloys and Compounds, 187 (1992) 181–192
JALCOM 297

Synthesis of tantalum tellurides: the crystal structure of Ta_2Te_3

Matthias Conrad and Bernd Harbrecht
Institut für Anorganische Chemie, Universität Bonn, Bonn (Germany)

(Received March 14, 1992)

Abstract

Ta_2Te_3 was prepared by reducing $TaTe_2$ with tantalum at 1350 K in a sealed molybdenum crucible. Ta_2Te_3 disproportionates above 1420 K yielding the ditelluride and as yet unknown Ta_6Te_5. The stability limit for the substitutional sesquitellurides $Nb_xTa_{2-x}Te_3$ is reached at $x \approx 1$. The novel layered-type structure of Ta_2Te_3 ($C\,2/m$, $N=4$; $a=2049.5(3)$ pm, $b=349.96(4)$ pm, $c=1223.7(2)$ pm, $\beta=143.74(1)^0$ (Guinier), $N(I_0)=762$ with $I_0>2\sigma(I_0)$, 32 variables, $R=0.032$) can be considered a stuffed variant of a molybdenite structure type. It consists of corrugated layers $^2_\infty$(Te–$Ta_{4/3}$–Te) which, according to the shortest interlayer contacts Te–Te (372.9 pm), order via van der Waals interactions. Extended homonuclear bonding regions (297.1 pm $\leq d_{Ta-Ta} \leq$ 309.7 pm) within the metal layers contribute to the stability of the metallic sesquitelluride.

1. Introduction

The recent discovery of Ta_2Se, with its unique layered-type structure [1] encouraged us to reinvestigate preparatively the binary system Ta–Te in order to unravel the phase relations in the region $1/3<x(\text{Ta})<1$. According to, *e.g.* Greenwood and Earnshaw [2], there exist two tellurides richer in metal than $TaTe_2$ [3], $Ta_{1+x}Te_2$ [3] and TaTe [4, 5]. Information about such reduced tellurides, however, is sparse and conflicting [3, 6].

Recently several reports have appeared about novel metal-rich ternary tantalum tellurides with unexpected structures. Whereas $MTaTe_2$ (M = Co, Ni) [7, 8] and $Ni_3Ta_2Te_5$ [8] belong to the group of layered-type compounds the most reduced tantalum telluride Ta_4SiTe_4 so far produced has all the features of a complex quasi-one-dimensional material [9, 10]: square anti-prismatic Ta_8 units — each stabilized by an incorporated Si atom — are condensed to columns via common "square" faces. The remaining valencies of the metal columns are saturated by Te atoms located above peripheral triangular prism faces according to $^1_\infty(Ta_{8/2}SiTe_4)$. Interestingly, the structures of the new binary tellurides Ta_2Te_3 [11] and Ta_6Te_5 [11] show strong similarities to those of the ternaries with respect to the importance of metal clustering and weak bonding interactions Te–Te for the architecture of the solids. This report focuses on the synthesis and phase relations of reduced tantalum tellurides and on the crystallographic structure of the first layered sesquitelluride.

0925-8388/92/$5.00

2. Experimental details

2.1. Preparation and phase relations

Well-crystallized, lubricant-like Ta_2Te_3 was prepared from a 3:1 mixture of $TaTe_2$ and Ta at 1150–1410 K within 1–8 days. The reactants were placed either in alumina crucibles inside previously outgassed quartz glass ampoules or in sealed Mo crucibles which were heated in a vacuum ($p < 10^{-3}$ Pa). Since the tellurides are slightly air sensitive they were handled in a glove box and stored in sealed ampoules; otherwise, traces of Ta_2O_5 were identified after reheating by comparison with the Guinier patterns of the respective samples with that of Ta_2O_5 (Alpha Ventron).

$TaTe_2$ was prepared from the elements (Ta: Aldrich, 99.9%, Te: Fluka, 99.999%) in evacuated sealed quartz glass tubes at 1200 K within 1 day, whereas in agreement with ref. 6 the presence of excess Ta at similar conditions led to severe attack of the silica tubes. Ta_2O_5 and Ta_4SiTe_4 [10] were identified as major contaminants. With the use of an additional alumina crucible Ta_2Te_3 of minor crystallinity was obtained. In the course of establishing reliable conditions for preparing single-phase Ta_2Te_3 we also noticed that Mo crucibles were not inert enough for reactions starting with the elements: the formation of Ta_2Te_3 seems to be suppressed. Energy dispersive analysis of X-rays (EDX: EDX AN 10000, Link) in a scanning electron microscope (SEM: stereoscan 360, Cambridge Instruments) indicated that the samples contained molybdenum as a second metal. In contrast to these observations, EDX showed no Mo/Ta exchange in samples of Ta_2Te_3 which were prepared from tantalum and $TaTe_2$ in Mo crucibles, even though $TaCl_5$ was present.

In accordance with ref. 6 and in opposition to ref. 3 our experiments do not indicate any noticeable insertion of additional Ta in $TaTe_2$. Mixtures somewhat richer in Ta than those for $TaTe_2$ yielded products containing both phases, $TaTe_2$ and Ta_2Te_3. In addition, lattice parameters of $TaTe_2$ (see Table 1) coexisting with $TaTe_4$ [12, 13] do not vary significantly from those of $TaTe_2$ coexisting with the sesquitelluride. There are also no hints of any incorporation of excess Ta in layered-type Ta_2Te_3: further reduction of $TaTe_2$ leads to Ta_6Te_5 [11], another binary not so far mentioned, which is also formed together with $TaTe_2$, when Ta_2Te_3 is heated above 1420 K. The disproportionation of Ta_2Te_3 takes place in the solid state. This result came from a series of heating experiments of Ta_2Te_3, in which the temperature was increased stepwise in 10 K increments from 1400 to 1460 K.

We also performed reactions in order to study the phase relations of the ternary system Nb–Ta–Te in the section $[n(\mathrm{Ta})+n(\mathrm{Nb})]/n(\mathrm{Te})=2{:}3$. A binary niobium sesquitelluride does not form under the chosen preparative conditions. However, Nb substitutes for Ta in $Nb_xTa_{2-x}Te_3$ up to $x \approx 1$. Outside the stability limit ($x > 1$) two additional phases with $NbTe_2$-type [3] and Nb_3Te_4-type [14] structures occur.

TABLE 1

Lattice parameters of tantalum tellurides (Guinier data, Cu $K\alpha_1$ radiation, internal standard: silicon)

$TaTe_2$	$a = 1923.7(3)$ pm $b = 363.50(7)$ pm $c = 934.5(2)$ pm $\beta = 134.16(1)°$
Ta_2Te_3 [a]	$a = 2049.5(3)$ pm $b = 349.96(4)$ pm $c = 1223.7(2)$ pm $\beta = 143.74(1)°$
$NbTaTe_3$ [a]	$a = 2061.3(3)$ pm $b = 350.63(4)$ pm $c = 1230.6(3)$ pm $\beta = 144.17(1)°$
Ta_6Te_5	$a = 1162.5(4)$ pm $b = 1937.9(6)$ pm $c = 2606.2(9)$ pm

[a]The unconventional setting was chosen in order to emphasize the metrical relationship between Ta_2Te_3 and $TaTe_2$. The conventional monoclinic C-centred cell ($a' = 1449.4$, $b' = 349.96$ and $c' = 1285.8$ pm, $\beta' = 127.26°$) is obtained by the transformation $\mathbf{a}' = -\mathbf{a} - 2\mathbf{c}$, $\mathbf{b}' = \mathbf{b}$, $\mathbf{c}' = \mathbf{a} + \mathbf{c}$.

2.2. *X-ray diffraction and structure calculation*

The samples were examined by means of X-ray powder diffraction in a vacuum Guinier camera (FR 552, Enraf Nonius, Delft, NL) using monochromatized Cu $K\alpha_1$ radiation. Silicon was admixed to the samples as a standard [15]. The diffraction patterns were indexed by consideration of calculated intensities (LAZY PULVERIX [16]). The parameters of $TaTe_2$ were taken from the literature [3]. The intensity calculations for Ta_2Te_3, $Nb_xTa_{2-x}Te_3$ and Ta_6Te_5 were based on parameters as obtained from single-crystal structure refinements. Lattice parameters of four tellurides are listed in Table 1. Table 2 contains measured and calculated $\sin^2\theta$ values and calculated and estimated relative intensities of Ta_2Te_3.

Nine slat-shaped crystals of Ta_2Te_3 were selected from samples prepared with I_2 or $TaCl_5$ as transport agent. Weissenberg (Cu $K\alpha$) and precession (Mo $K\alpha$) photographs pointed to a monoclinic C-centred lattice without further extinctions. The exposures of all crystals showed additional reflections due to a systematic twinning with m perpendicular c^* as a twinning element. The intensities of the individuals varied within about 5–100% relative to each other.

A crystal of a sample with nominal composition $n(Ta):n(Te) = 3:4$ was chosen for data collection (monochromatized Mo $K\alpha$ radiation; CAD4, Enraf–Nonius). As estimated from corresponding, spatially separated reflections of layers $h0l$ and $h1l$ the ratio of the volumes of the two individuals was about 10. Data reduction and structure calculations were performed with the program SDP PLUS (B. Frenz *et al.* [25]). The structure was solved by

TABLE 2

Guinier data (Cu $K\alpha_1$) for Ta_2Te_3 ($\sin^2\theta<0.2$)

h k l	$Sin^2\theta\times10^5$		I_{rel}	
	Calculated	Observed	Calculated	Estimated
0 0 1	1133	1135	100	10
2 0 0	1615	1623	3	1
2 0 −2	1783	1785	2	1
4 0 −1	3231	3231	2	1
6 0 −3	5099	5102	12	5
1 1 0	5248	5249	3	2
1 1 −1	5290	5331	2	2
3 1 −1	6339	6341	11	5
6 0 −4	6484	6481	8	4
1 1 1	7471	7469	17	5
1 1 −2	7597	7598	3	1
3 1 0	8478	8477	15	4
5 1 −2	8563	8565	16	6
5 1 −3	8774	8770	18	6
3 1 −3	8857	8849	61	8
8 0 −4	9065	9073	7	4
6 0 −1	9125	9128	28	3
8 0 −3	9861	9867	7	4
6 0 −5	10134	10118	2	1
0 0 3	10194	10187	4	1
8 0 −5	10534	10537	14	5
5 1 1	10618	10627	19	5
2 0 −4	11012	11017	8	3
1 1 2	11960	11960	19	5
7 1 −4	12215	12210	3	3
4 0 −5	12964	12949	6	3
3 1 −4	13513	13509	11	4
10 0 −5	14164	14177	1	1
8 0 −6	14268	14262	10	3
6 0 0	14535	14537	8	2
7 1 −5	14775	14753	7	3
5 1 0	14938	14932	9	3
9 1 −4	16411	16407	22	8
0 0 4	18122	18125	2	1
7 1 −1	18127	18125	2	1
9 1 −3	18297	18300	3	2
2 0 −5	19025	19033	10	3
0 2 0	19377	19376	18	8

direct methods in space group type $C\ 2/m$. After refinements of the scale factor, positional parameters and isotropic displacement parameters with all $|F_0|$ for which $I_0>2\sigma(I_0)$, an empirical absorption correction [17] was applied. Merging of data led to $R_{int}(F_0)=0.038$ compared with $R_{int}(F_0)=0.049$ obtained after an absorption correction based on azimuthal scans of six reflections. Subsequently, anisotropic displacement parameters and a secondary extinction parameter were included in the refinements. $\Sigma w(|F_0|-|F_c|)^2$, $w=[\sigma^2(F_0)+C^2|F_0|^2]^{-1}$, was minimized. Due to perfect superposition of $I_0(0kl)$ of both individuals 16 $|F_0(0kl)|$ were omitted in the final calculations. The highest relative residual electron density $\rho_{max}/\rho_{max}^{(Te)}=0.015$ is 83 pm distant from Ta1; residual charge density in the van der Waals gaps was negligible. Since the crystal was selected from a sample richer in tantalum than Ta_2Te_3, additional insertion of Ta in Ta_2Te_3 can be ruled out. Further details of data collection and structure calculations are given in Table 3. Positional and displacement parameters are listed in Tables 4 and 5. Table 6 contains characteristic interatomic distances.

2.3. *The structure of* Ta_2Te_3

Ta_2Te_3 forms a new structure type with monoclinic symmetry. It is built up from five crystallographically distinct atoms, Ta1, Ta2, Te1, Te2 and Te3.

TABLE 3

Data collection and structure calculation of Ta_2Te_3

Space group type	*C* 2/*m* [No. 12]
Z	4
a (pm)	2047.1(5)
b (pm)	349.5(2)
c (pm)	1222.4(3)
β	143.8(1)°
Crystal size (mm^3)	$0.05\times0.3\times0.09$
X-ray, monochromator	Mo Kα, graphite
Min. transmission (%)	28.0
θ-Range, scan type	1 − 30°, Ω–2θ
Octants measured	$+/-h$, k, $+/-l$
Reflections measured	2010
Independent reflections	827
Independent reflections with $I_0>2\sigma(I_0)$	762
$R_{int}(F_0)$	0.038
Number of variables	32
$R(F_0)/R_w(F_0)$	0.032/0.050
ESD	1.10
Secondary extinction coefficient	7.17×10^{-7}
Residual charge density (e pm^{-3})	3.8×10^{6}

TABLE 4

Positional parameters and equivalent isotropic displacement parameters B_{eq} (10^4 pm^2) of Ta_2Te_3

Atom	Position	*x*	*y*	*z*	B_{eq}
Ta1	4i .*m*.	0.41688(3)	0	0.97715(4)	0.344(9)
Ta2	4i .*m*.	0.23010(2)	0	0.07108(4)	0.361(9)
Te1	4i .*m*.	0.43128(4)	0	0.22389(7)	0.45(1)
Te2	4i .*m*.	0.18734(4)	0	0.66164(7)	0.46(2)
Te3	4i .*m*.	0.10522(4)	0	0.23811(7)	0.46(2)

TABLE 5

Anisotropic displacement parameters U_{ij} (pm^2) of Ta_2Te_3 ($U_{12}=U_{23}=0$)

Atom	U_{11}	U_{22}	U_{33}	U_{13}
Ta1	48.3(6)	46(3)	56.5(6)	46.6(3)
Ta2	51.9(6)	44(3)	57.9(6)	47.8(3)
Te1	62(1)	49(4)	72(1)	57.0(6)
Te2	59(1)	45(4)	47(1)	37.5(6)
Te3	70(1)	41(4)	55(1)	48.5(6)

TABLE 6

Characteristic interatomic distances (pm) of Ta_2Te_3

Ta1–Ta1 1×	297.1(1)	Ta2–Ta1 2×	309.7(1)
–Ta1 2×	349.5(1)	–Ta2 2×	300.4(1)
–Ta2 2×	309.7(1)	–Ta2 2×	349.5(1)
–Te1 1×	278.4(1)	–Te1 2×	278.4(1)
–Te2 1×	277.8(1)	–Te1 1×	283.5(1)
–Te3 2×	287.2(1)	–Te2 2×	277.0(1)
–Te3 2×	287.4(1)		
Te1–Ta1 1×	278.4(1)	Te2–Ta1 1×	277.8(1)
–Ta2 2×	278.4(1)	–Ta2 2×	277.0(1)
–Ta2 1×	283.5(1)	–Te1[a] 2×	372.9(2)
–Te1 2×	349.5(1)	–Te2 2×	349.5(1)
–Te2[a] 2×	372.9(2)	–Te3[b] 2×	376.7(1)
–Te3[b] 2×	384.2(1)		
Te3–Ta1 2×	287.2(1)		
–Ta1 2×	287.4(1)		
–Te1[b] 2×	384.2(1)		
–Te2[b] 2×	376.7(1)		
–Te3[b] 1×	346.2(2)		
–Te3 2×	349.5(1)		

[a]Te–Te distances between layers.
[b]Te–Te distances within one layer.

All atoms are located in mirror planes perpendicular to the unique axis at $y=0$, 1/2 modulo 1. They occupy Wyckoff position 4i, $x0z$ of space group type $C\ 2/m$.

Ta atoms are arranged in corrugated layers running parallel (001). They are sandwiched by puckered, close-packed-like layers of Te atoms (mean distance $<d(\text{Te–6Te})> = <375.5$ pm$>$). The stacking sequence of two adjacent slabs is AB. The shortest Te–Te interslab distance is 373 pm compared with 360 pm for CdI_2-type related $TaTe_2$ [3]. Strong attractive interactions are obviously restricted to atoms of single quasi-two-dimensional arrays $^2_\infty(Ta_{3/4}Te_2)$. A stacking of the slabs by van der Waals interactions gives an explanation for the easy cleavage of the crystals. A view of the structure is shown in Fig. 1.

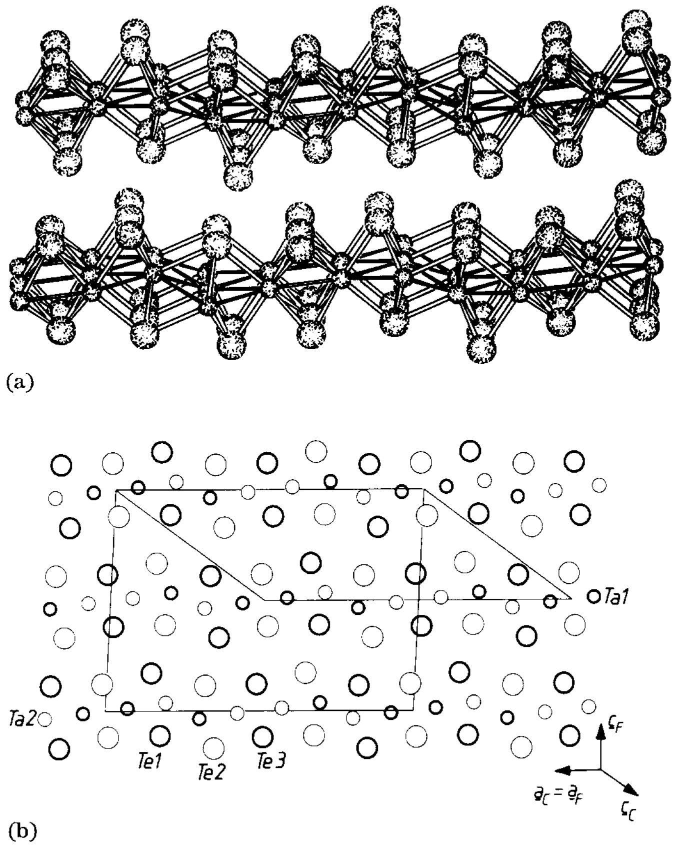

Fig. 1. The layered structure of Ta_2Te_3 (large circles Te, small circles Ta): (a) perspective view along b; (b) projection on to (010) (thin circles $y=0$, bold circles $y=1/2$; for different settings see text).

Since there are no close Te–Te contacts within the slabs (all approximately larger than 346.2 pm) we could expect Ta to be in oxidation state +3. In this case, two residual electrons per Ta atom can enter into homonuclear bonds. Such extended bonding regions are clearly indicated by the arrangement of the Ta atoms within layers consisting of edge-fused hexagons and rhombi. As seen from Fig. 2 short distances (less than 349.5 pm $=b$) range from 297.1 pm to 309.7 pm. However, Ta1 and Ta2 differ significantly in their coordinations and bonding interactions: (i) Ta1 has three Ta neighbours at <305.5 pm>, Ta2 has four at <305.0 pm>; (ii) Ta1 is distorted trigonal prismatically coordinated by six Te (<284.2 pm>), Ta2 has a distorted square pyramidal configuration of Te (<278.9 pm>) (Fig. 3). The consideration of the specific coordinations of Ta1 and Ta2 points to a kind of disproportionation with rather more electron density available for homonuclear interactions at Ta2 than at Ta1. However, if two electrons were localized between two next Ta1 (297.1 pm) there would remain exactly one electron

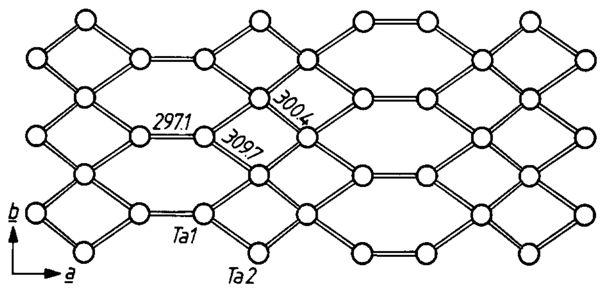

Fig. 2. Projection of a single tantalum layer on to (001) (distances in picometres).

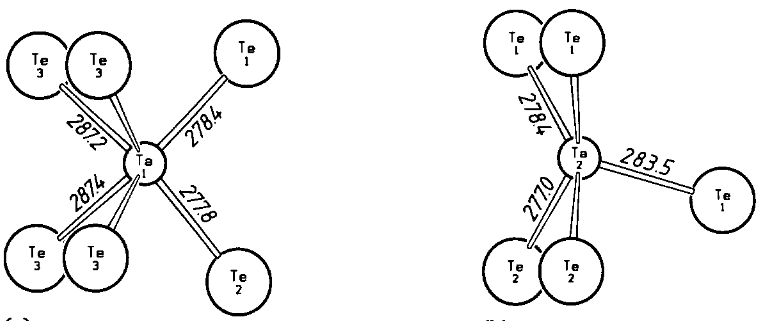

(a) (b)

Fig. 3. Tellurium coordination about: (a) Ta1; (b) Ta2 (distances in picometres).

for every other short contact Ta–Ta, as emphasized by lines in Fig. 2. Then Ta1 and Ta2 would each contribute two electrons to the extended homonuclear bonding regions.

As mentioned above, the three non-equivalent Te atoms are strongly bonded only to Ta atoms of a single layer. Te2 (<277.3 pm>) is coordinated by three Ta atoms similar to Te (<281.0 pm>) in $TaTe_2$ [3]. Te1 and Te3 have four Ta neighbours in a different configuration (Fig. 4) at <279.7 pm> and <287.3 pm> respectively. Interestingly, the shortest Te–Te contacts appear between Te3 (346.2 pm), which are about 8 pm further away from four Ta than Te1. Because Te3 is strongly bonded exclusively to Ta1 we hesitate to conclude that heteronuclear bonds are weakened at the cost of the formation of weak covalent interactions Te3–Te3. The valence electron concentration available for metal–metal bonds would then be higher for Ta1 than for Ta2. Since shorter Te3–Ta1 bonds were intrinsically associated with closer contacts Te3–Te3 at given distances Ta1–Ta1 and without significant splitting of distances Te3–Ta1, another solution to the local minimization of potential energy seems to be more likely. The suspiciously short distance Te3–Te3 together with the relatively large distance Te3–Ta1, reflect the balance between homonuclear repulsive (Te3–Te3) and heteronuclear attractive (Te3–Ta1) interactions.

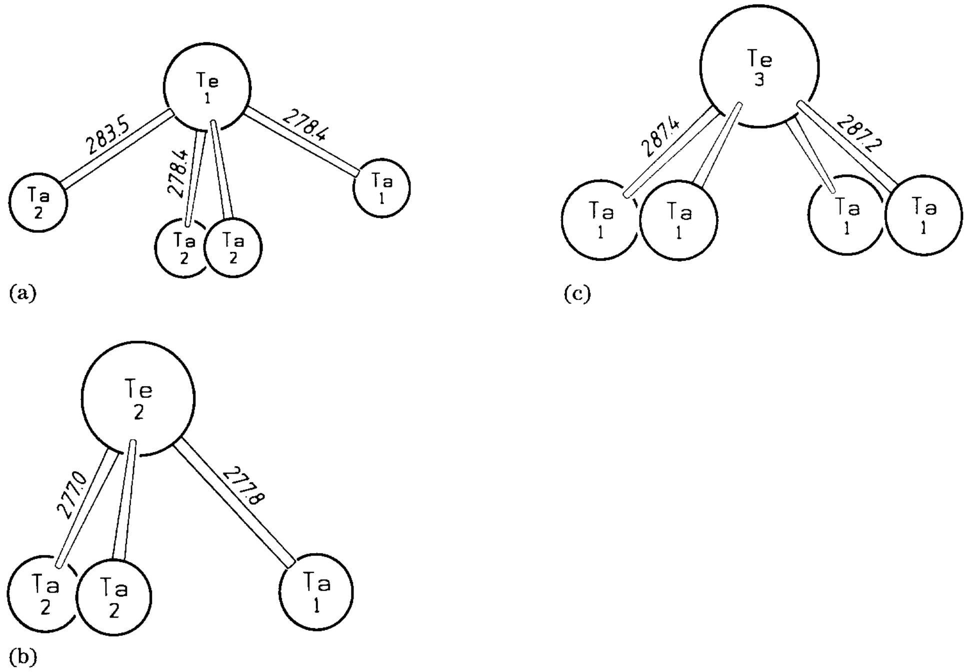

Fig. 4. Tantalum coordination about: (a) Te1; (b) Te2; (c) Te3 (distances in picometres).

At this point it is worth mentioning that all three coordinations about Te (Fig. 4) can be considered as fragments of a tricapped trigonal prismatic Ta_9Te polyhedron. Such tetrakaidecahedra and/or fragments thereof around atoms of an electronegative main group element are a common topological feature of all binary and ternary metal-rich chalcogenides and many pnictides containing a metal of group 4 or 5 as a major component. This feature appears irrespective of composition and irrespective of the structural complexity of the materials which are composed of b.c.c. fragments, centred metal icosahedra or even centred M_9 tetrakaidecahedra themselves. New examples are $Nb_{11-x}Ta_xS_4$ [18] and Ta_2Se [1] (b.c.c. fragments), Ta_3S_2 [19, 20] and $Au_xTa_{15-x}S_2$ [21] (centred metal icosahedra), and $M_2Ta_{11}Se_8$ [22] (MTa_9 tetrakaidecahedra, M≡Fe, Co, Ni), $M_{2-x}Nb_8S_{4+x}$ (M≡Co, Ni) [23, 24].

As seen from Fig. 5 the structure of Ta_2Te_3 can be related to a dichalcogenide structure type, MCh_2, in which metal atoms have a trigonal prismatic coordination. The composition of a sesquitelluride is reached if one-third of the empty trigonal prismatic sites within the MCh_2 slabs are occupied by M atoms. An ordered distribution of M atoms in the manner depicted in Fig. 5(b) would require four crystallographically distinct M atoms; only two are necessary for a pattern as shown in Fig. 5(c). This agrees qualitatively well with a projection of a $Ta_{4/3}Te_2$ slab, as present in Ta_2Te_3.

A stacking vector nearly perpendicular to a_C and b_C is obtained for Ta_2Te_3 by the following transformations: $a_F = a_C$, $b_F = -b_C$, $c_F = -a_C - 2c_C$.

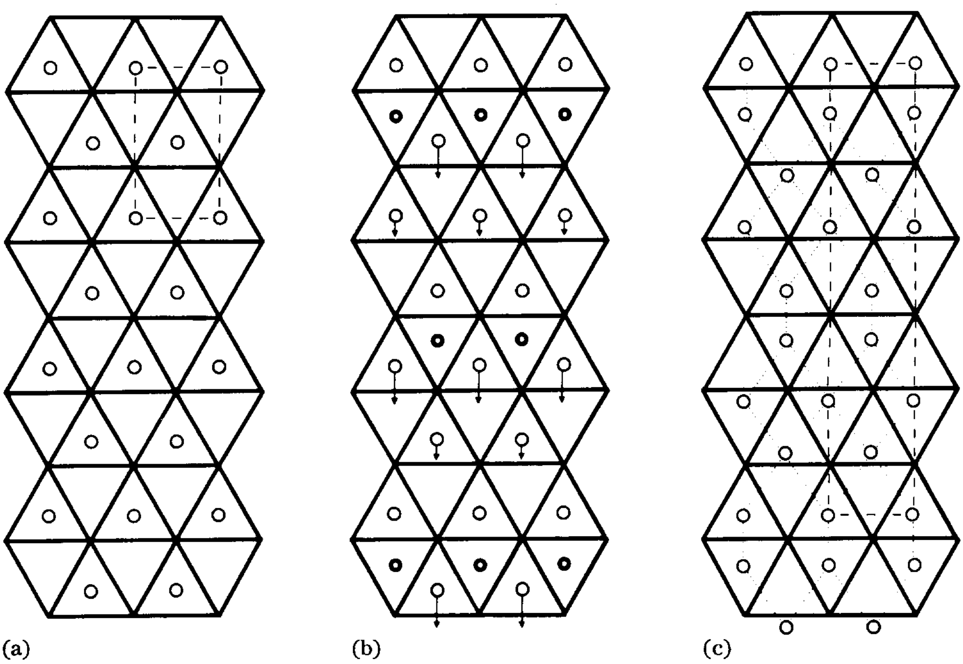

Fig. 5. Schematic structural relationship between slabs of MoS_2 and Ta_2Te_3: (a) projection of an MoS_2 slab; (b) 1/3 of empty trigonal prismatic sites are additionally filled with M atoms; (c) the idealized pattern of $Ta_{4/3}Te_2$ slabs.

Subscripts C and F refer to the chosen C-centred lattice and to an unconventional F-centred lattice ($a = 2049.5$ pm, $b = 349.96$ pm, $c = 1449.4$ pm, $\beta = 93.01°$) respectively.

If we neglect a shear deformation of less than 3° and ignore atom shifts of some 50 pm, we arrive at a fictitious orthorhombic structure of Ta_2Te_3 without corrugated metal layers and without any differentiation between Te1 and Te2. This can be described as space group type *F mmm*: eight Ta1, eight Ta2 at 8g 2*mm* (x00), eight Te1 together with eight Te2 at 16n .*m*. (x0z) and eight Te3 at 8i *mm*2 (00z).

These relationships reveal that the unique layered-type structure of Ta_2Te_3 can be considered topologically as a stuffed variant of a MoS_2-type structure. A symmetry relation between the two structure types does not exist, however. The uncovered symmetry relation between the real structure of Ta_2Te_3 (*C* 2/*m*) and the fictitious one without corrugated layers (*F mmm*) obeys the group–subgroup relationship $F\,mmm \xrightarrow{t2} C\,2/m$. This provides a possible rationalization for the observed twinning of the crystals. In view of this relationship the twinning could be the result of a displacive phase transition which might occur when the material is cooled down to ambient temperature. However, since the bonding interactions in the fictitious flat layered structure differ drastically from those in the real, corrugated layered structure and since the volume ratio of the differently oriented domains varies arbitrarily from crystal to crystal, it seems more likely that the twinning appears due to weak interactions between adjacent $Ta_{3/4}Te_2$ layers already formed during crystal growth.

3. Conclusions

We have established the existence of two previously undiscovered binary tantalum tellurides Ta_2Te_3 and Ta_6Te_5. In the sesquitelluride tantalum can be partially replaced by niobium, yielding substitutional phases of composition $Nb_xTa_{2-x}Te_3$ with $0 < x \leq 1$. The first layered-type structure of a sesqui-chalcogenide has been determined from X-ray diffraction data obtained from a twinned crystal of Ta_2Te_3. Attractive Ta–Ta interactions contribute to the stability of the telluride which orders in one direction via van der Waals interactions. The topological relationship between an MoS_2-type structure and that of Ta_2Te_3 is elucidated.

Acknowledgments

The support of this study by the Deutsche Forschungsgemeinschaft and by the Fonds der Chemischen Industrie im Verband der Chemischen Industrie is gratefully acknowledged.

References

1 B. Harbrecht, *Angew. Chem., 101* (1989) 1696; *Int. Ed. Engl., 28* (1989) 1660.
2 N. N. Greenwood and A. Earnshaw, *Chemie der Elemente*, Verlag Chemie, Weinheim, 1988, p. 1271.
3 B. E. Brown, *Acta Crystallogr., 20* (1966) 264.
4 L. H. Brixner, *J. Inorg. Nucl. Chem., 24* (1962) 257.
5 E. Revolinsky, B. E. Brown, D. J. Beerntsen and C. H. Armitage, *J. Less-Common Met., 8* (1965) 63.
6 K. Selte, E. Bjerkelund and A. Kjekshus, *J. Less-Common Met., 11* (1966) 14.
7 J. L. Huang and B. G. Huang, *Acta Crystallogr., Sect. A, 46* (Suppl.) (1990) C-287.
8 W. Tremel, *Angew. Chem., Int. Ed. Engl., 103* (1991) 900.
9 J. Li, R. Hoffmann, M. E. Badding and F. J. DiSalvo, *Inorg. Chem., 29* (1990) 3943.
10 M. E. Badding and F. J. DiSalvo, *Inorg. Chem., 29* (1990) 3952.
11 M. Conrad and B. Harbrecht, paper presented at the *Tenth Int. Conf. on Solid Compounds of Transition Elements, Münster, May 21–25, 1991.*
12 E. Bjerkelund and A. Kjekshus, *J. Less-Common Met., 7* (1964) 231.
13 K. D. Bronsema, S. van Smaalen, J. L. de Boer, G. A. Wiegers and F. Jellinek, *Acta Crystallogr., Sect. B, 43* (1987) 305.
14 K. Selte and A. Kjekshus, *Acta Crystallogr., 17* (1964) 1568.
15 R. D. Deslattes and A. Henins, *Phys. Rev. Lett., 31* (1973) 972.
16 K. Yvon, W. Jeitschko and E. Parthé, *J. Appl. Crystallogr., 10* (1977) 73.
17 N. Walker and D. Stuart, *Acta Crystallogr., Sect. A, 39* (1983) 158.
18 X. Yao and H. F. Franzen, *J. Solid State Chem., 86* (1990) 88.
19 S.-J. Kim, K. S. Najundaswamy and T. Hughbanks, *Inorg. Chem., 30* (1991) 159.

20 H. Wada and M. Onoda, *Mater. Res. Bull.*, *24* (1989) 191.
21 B. Harbrecht and V. Wagner, *Gemeinsame Tagung Arbeitsgemeinschaft Kristallographie*, München, 1991.
22 B. Harbrecht, *J. Less-Common Met.*, *141* (1988) 59.
23 B. Harbrecht, Habilitationsschrift, University of Dortmund, 1989.
24 M. Conrad, Diplomathesis, University of Dortmund, 1990.
25 B. A. Frenz, in H. Schenk, R. Olthof-Hazekamp, H. van Koningsveld and G. C. Bassi (eds.), *Computing in Crystallography*, Delft University Press, Delft, NL, 1978, p. 564.